EFFECT OF PITTING CORROSION ON FATIGUE AND CRACK GROWTH BEHAVIOR OF BOTH ALUMINUM ALLOY 2024-T62 AND ITS PANEL

J.Z.LIU, B.CHEN, X.B.YE, B.R.HU, C.F.DING, and X.R.WU
Beijing Institute of Aeronautical Materials, Beijing 100095, China

Keywords: *Pitting corrosion, Aluminum alloy, Fatigue, Crack Growth, Life prediction*

Abstract

As part of study on remaining life and residual strength of corroded aluminum alloy structures, in this paper effects of pitting corrosion on fatigue, large and small crack behavior of aluminum alloy 2024-T62 and on fatigue of the material panel with multiple holes were studied experimentally. Fatigue lives of the corroded material and panel were predicted and compared with experimental results.

1 Introduction

Corrosion damage is often found on aluminum alloy aircraft structures subjected to fatigue loading. Although many aspects of this problem have been studied extensively over the past 20 years, there is no generally applicable model available to predict the service life of corroded aluminum alloy structures, and design against fatigue in the presence of corrosion [1-5]. Several investigators have studied effect of corrosion pits on fatigue behavior of aluminum alloys, and predicted reasonably the fatigue life of corroded specimen using the commercial crack growth software AFGROW, NASGRO, etc by assuming a pre-corrosive pit as an initial small crack [2,5]. However, possible effect of small crack behavior on the prediction was not studied. Moreover, few studied [6] on small corrosive fatigue crack behavior of aluminum alloy have carried out so far.

As part of study on remaining life and residual strength of corroded aluminum alloy structures, effects of pitting corrosion on fatigue and crack growth behavior of aluminum alloy 2024-T62 were carried out experimentally in lab air. Especially, the effects of pitting corrosion on small fatigue crack behavior in lab air and corrosive solution were investigated. Effect of pitting corrosion on small crack growth threshold behavior was evaluated. Moreover, fatigue behavior of the corroded aluminum alloy panel with multiple collinear holes was also studied. Finally, fatigue lives of the corroded material and panel were predicted.

2 Material, Specimen and Testing Procedures

Alclad 2024-T62 aluminum alloy sheet with the thickness of 2mm is selected. Its chemical composition are Cu 4.64%, Mg 1.49%, Mn 0.68%, Si <0.5%, Fe <0.5%, Zn <0.25%, Ti <0.15%, Cr <1%, other <0.15%, and Al balance. Static tensile properties of the material are given in Table 1.

The specimen with tangentially blending fillets between the uniform test section and the ends, as shown in Fig.1, is selected for fatigue testing of pre-corroded material. The standard M(T) specimen is used for large crack growth testing in laboratory air and aqueous 3.5% NaCl. The Single-edge-notch tension (SENT) specimen with the semi-circular notch radius of 3.2mm (See Fig.2) is used for small crack behavior testing in lab air and aqueous 3.5% NaCl. The extended compact tension (EC(T)) specimen (Fig.3) is selected to perform physical small crack threshold tests. The panel with 5 collinear holes (Fig.4) is used to test the effect of prior corrosion on fatigue behavior of aluminum alloy structure. All coupons and panels were machined with the loading axis parallel to the longitudinal direction of the extrusion. No machining is performed along the thickness direction of the material. The Alclad layer on two surfaces of material sheet remains unchanged on the surfaces of the specimens.

Table 1. Static tensile properties of the material

E（GPa）	σ_b（MPa）	$\sigma_{0.2}$（MPa）	δ_5%
71	451	400	7.2

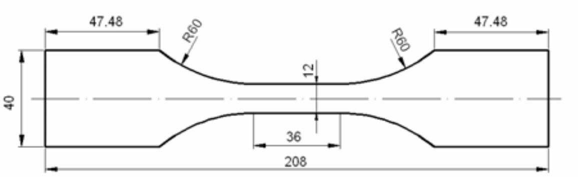

Fig.1 fatigue specimen with uniform section

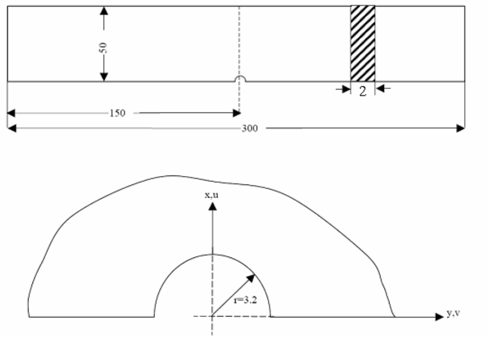

Fig.2 SENT specimen

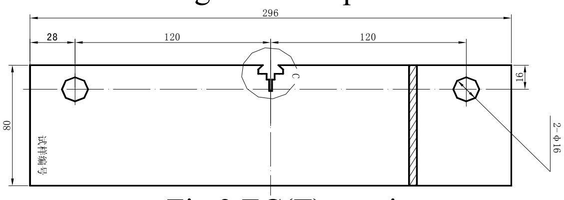

Fig.3 EC(T) specimen

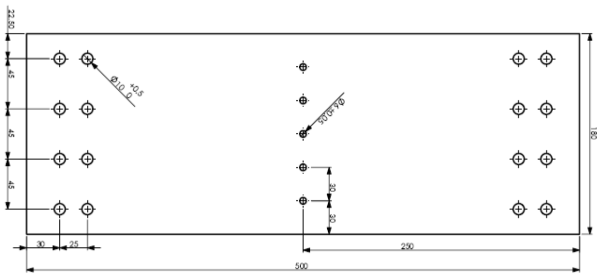

Fig.4 Panel with 5 collinear holes

Many fatigue specimens were immersed in 3.5% NaCl solution for 12h, 24h, 48h, 96h, 120h and 240h, respectively to get different prior corrosions. All the panels were immersed in 3.5% NaCl solution for 240h before testing. Some M(T) specimens were immersed in the solution for 24 h and 240h, respectively.

A small sealed plastic chamber with 3.5% NaCl corrosive solution was used for corrosion fatigue and crack growth experiments. A special technique was developed for getting pre-corrosive pits with the diameters of 100μm ~ 300μm in a specified position of root surface at semi-circular notch of SENT specimen by prior corrosion for 240h. Some SENT specimens for small crack tests were carefully treated using this technique to make a small pre-corrosive pit (about 200μm) before small crack testing.

All small and large crack growth tests were carried out on MTS closed loop servo-hydraulic testing machine. Except that it is about 25Hz for crack growth threshold testing, the frequencies for all other tests are about 10Hz. In the cyclic loading, the sinusoidal wave was selected. After the fatigue testing, the corrosion pit depths and morphology were analyzed to determine the extent of corrosion damage.

Crack length measurement was performed using the plastic replica method [7] for small crack testing with naturally initiation crack in laboratory air. A Questar long distance optical microscope system was established to measured small crack growth for corroded SENT specimens in both lab air and aqueous 3.5% NaCl. SEM was used to determine the size and shape of pre-corrosive pits.

Length measurement for large crack growth tests was conducted by means of a travel optical microscopy with the magnification ×20. The constant K_{max}/increasing K_{min} method [8] was used to test the physical small-crack threshold. In the testing, the compliance method was used to obtain crack length.

The secant method was used to calculate crack growth rates for both small and large cracks. Stress intensity factors (SIFs) for SENT specimen with small crack were calculated using the expressions of Newman et al [7]. The expression for M(T) specimen in ASTM standard E647 was used to calculate the stress intensity factors.

Fatigue behavior tests of the corroded panel with 5 collinear holes were conducted in laboratory air under three loading stress levels at R=0.06. All the panels were immersed in 3.5% NaCl solution for 240h before the fatigue tests.

3 Experimental Results and Analyses

3.1 Effect of Corrosion Immersion Time on Pre-corrosive Damage

All specimens experienced pitting on the 2024-T62 alloy away from the clad layer at the machined uniform test section (i.e. the thickness surfaces). SEM investigation of pits after different prior immersion times revealed their irregular and complex morphology. Typical of morphologies of corrosive pit and its 3D view are shown in Fig.5 (a,b).Variation curve of average depth for pre-corrosive pits with the immersion time was obtained by fitting, which is showed in Fig.6. A relationship of power function between average depth of pre-corrosive pit and the immersion time can be found.

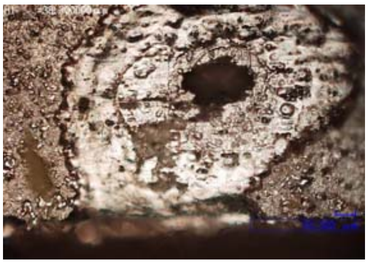

(a)

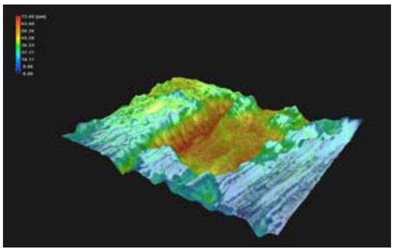

(b)

Fig.5 Typical of morphology of corrosion-pit （×350） and its 3D view

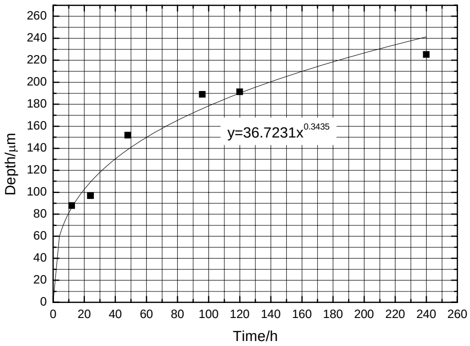

Fig.6 Variation of average depth of pre-corrosion pit with the immersion time

3.2 Effect of Pre-corrosive Damage on Fatigue S-N behavior

Comparisons among fatigue S-N curves for the corroded aluminum alloy at R=0.06 with different pre-corrosive times (0h、24h、96h、120h、196h and 240h) and at R=0.5 with the pre-corrosive times (0h 、 120h 、 240h) are shown in Fig.7(a, b), respectively. From the figures, an obvious effect of pre-corrosive damage on fatigue behavior is found. And fatigue properties decreases obviously with increasing pre-corrosive time. SEM fracture analyses of fatigue specimens show that all fatigue cracks initiate from corrosive pits.

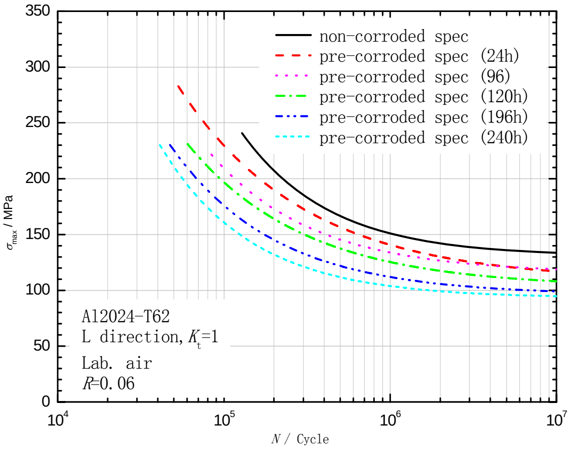

(a) R=0.06

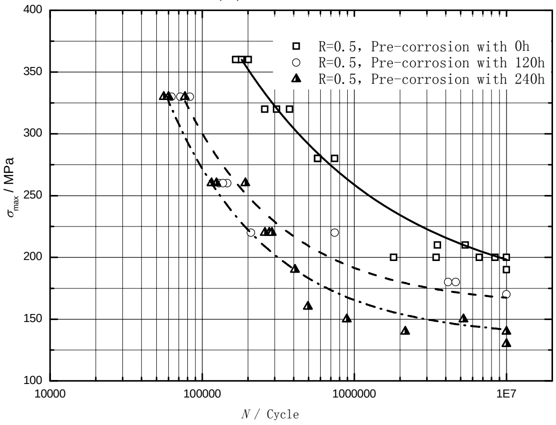

(b) R=0.5

Fig.7 Effect of pre-corrosion damage on fatigue S-N curves a) R=0.06, (b) R=0.5

3.3 Effect of Pre-corrosive Damage on Large Crack Growth Behavior

The relationships between wide range of crack growth rate *da/dN* (including crack growth threshold) and stress intensity factor range ΔK are shown in Fig.8(a,b) at R=0.5 and 0.06, respectively for the corroded material with different pre-corrosive times (0h, 24h, and 240h). From the figures, it can be found that the d*a/dN* data of large cracks from different pre-corrosive times is agreed well together at the different crack growth regimes. This shows that effect of pre-corrosive damage on large crack growth rates is not obvious.

3.4 Effect of Pre-corrosive Damage on Small Crack Behavior

For non-corroded SENT specimen, surface replicas taken early in life were used to locate where cracks were initiating and to identify the microstructural feature that caused the cracking.

It is found that small cracks initiated naturally from voids. All small cracks (<25μm) initiated below 20% of total fatigue lives. For pre-corroded SENT specimen, a Questar long distance optical microscope system was used to monitor and measure small crack growth in laboratory air and aqueous 3.5% NaCl. It is found that all small cracks initiated from pre-corrosion pits, initiation lives of small cracks (a≤60μm) are below 25% of total fatigue lives.

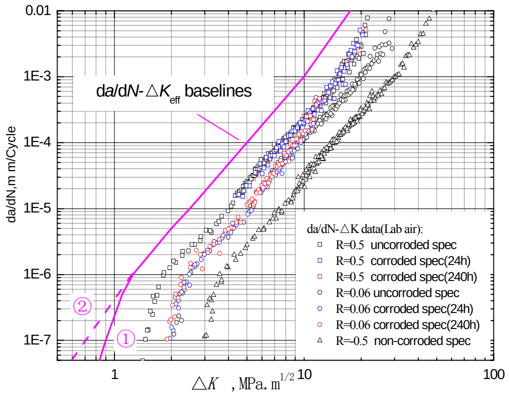

(a) The baselines for FASTRAN3.9 prediction

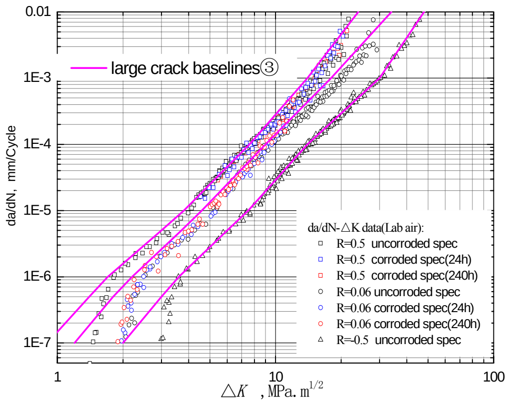

(b) The baselines for AFGROW prediction

Fig.8 Large crack growth-rate data of the corroded material with different pre-corrosion damage and the baselines used in different life prediction models

Comparisons among small and large crack growth rates from non-corroded and pre-corroded specimens in lab air and aqueous 3.5% NaCl are given in Fig.9 (a, b) for R=0.06 and –1, respectively. From the figures, the following useful results can be found: (1) At R=-1, large cracks in aqueous 3.5% NaCl grow a little faster than that in laboratory air. However, at R=0.06, large cracks grow almost at the same rates in this two environments. Effect of corrosion environment on large crack growth rates is small for this material. (2) For all small cracks that initiated naturally from the voids of the material in lab air at R=0.06, and initiated from pre-corrosive pits in lab air and aqueous 3.5% NaCl at R=-1 and 0.06, the small effect [7] is not found. However, small cracks that initiated naturally from the voids of the material at R=-1 showed an obvious small crack effect. (3) The small cracks that initiated from different conditions grow almost at the same rates. Effect of pre-damage on small crack growth behavior is not in existence. At two stress ratios, small cracks that initiated from pre-corrosive pits in lab air and aqueous 3.5% NaCl grow almost at the same ratios. Effect of environment on small cracks is not in existence for the material.

For Al2024-T3 in aqueous 1% NaCl and at a constant anodic potential of –700VSCE, Piascik [6] found that when exposed to Paris regime levels of crack tip stress intensity, small corrosion fatigue cracks (a≥100μm) exhibit growth rates similar to that observed for large cracks. This conclusion agrees with the present investigation. However, Piascik also found that in aqueous 1% NaCl and at a constant anodic potential of –700VSCE, small cracks which naturally initiated from constituent particle pits exhibit a factor of three increase in fatigue crack growth rates compared to lab air. This result does not agree with the present investigation. It maybe is concerned with the T6 treatment of the material that is thought to increase the properties of anti-corrosion.

3.5 Effect of Pre-corrosive Damage on Physical Small Crack Threshold Behavior

Constant K_{max}/increasing K_{min} tests were conducted for EC(T) specimen to obtain physical small crack growth threshold. Because the loading stress ratio R exceeds 0.9 near the threshold, the crack closure effects induced by plasticity, roughness on crack surface and corrosive production, etc. can be removed. The obtained threshold can be assumed to be physical small crack growth threshold $(\Delta K_{eff})_{th}$ [8]. The relationship data between da/dN and ΔK near the physical small crack growth threshold for the specimens with different pre-corrosive damages are given in Fig.10. From the Figure, no obvious effect of pre-corrosive damage is found on growth behavior at and near the physical small crack threshold.

3.6 Fatigue Behavior of the Corroded Panel with 5 Collinear Holes

Fatigue fracture of all the corroded panels was analyzed by SEM. Most of fatigue cracks are found to initiate from the corrosive pits at edges of holes. The obtained sizes of the corrosive pits, the loading stress levels at R=0.06 and the corresponding fatigue lives are given in Table 2. From Table 2, an obvious effect of pre-corrosive damage can be found on fatigue life of the panel with 5 collinear holes. Under the same loading stress level, the panel with the smallest sizes of the corrosive pits (and/or with few or no corrosive pits) is with the longest fatigue life, such as the panels, w1, w8, and w11.

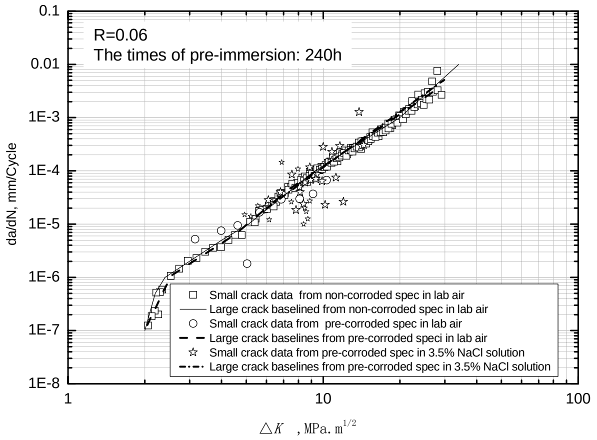

(a) R=0.06

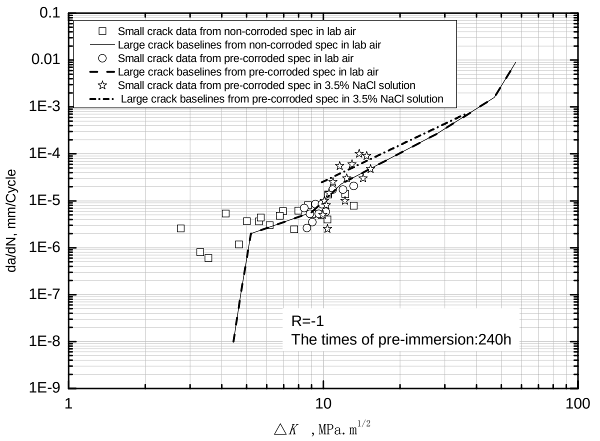

(b)R=-1

Fig.9 Comparisons among small and large crack growth rates from non- and pre-corroded specs in lab. air and aqueous 3.5% NaCl.

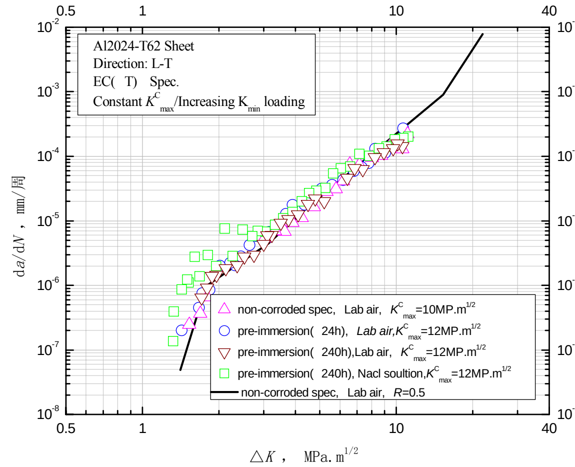

Fig.10 Effect of pitting corrosion time on physical small crack growth threshold behavior

4 Fatigue Life Predictions

FASTRAN3.9 software, which generally is used to predict total fatigue life of materials based on small crack theory [7], was used herein for predicting fatigue lives of corroded material. In order to make comparison, AFGROW software was also used in present investigation. Large crack growth baselines used in the predictions for FASTRAN3.9 and AFGROW are respectively shown in Fig.8 (a,b). Considering that the large crack data for rates nearby the growth threshold may be influenced by closure due to the load-shedding procedure [7], the dashed line (2) at the lower rate area in the Fig.8 (a) was estimated by trial-and-error to fit the endurance-limit behavior from the fatigue tests. The dashed line (2) was used to substitute the solid line (1) as the baseline in the predictions. In Fig.8(b) the baselines at different stress ratios used in AFGROW prediction were modified to account for “short crack” growth behavior by extending the middle part of the Paris regime below the threshold stress intensity as performed in other investigations [2,5].

In calculating fatigue lives, crack growth was assumed to begin during the first applied cycle with no crack initiation period included in the analysis. Such an assumption is assumed to be rational. As mentioned before, for small cracks that initiated from the pre-corrosive pits, the initiation lives of small cracks (a≤60μm) are below 25% of total fatigue lives. And the results from aluminum alloy 2024-T3, and 2524-T3 subjected to interrupted fatigue testing have also shown fatigue cracks emanating from pits at less than 15% of the total fatigue life [9].

Table2 Results from SEM analyses of fatigue fracture for the corroded panels
(Units of width and depth for corrosive pits from which fatigue cracks initiate: μm)

Spec. No.	Hole1		Hole2		Hole3		Hole4		Hole5		Testing results	
	Edge of left	Edge of right	Edge of left	Edge of right	Edge of left	Edge of right	Edge of left	Edge of right	Edge of left	Edge of right	Stress level	cycles
w1	little	little	little	—	little	—	—	122(d) 100(w)	118(d) 72(w)	little	110 /MPa	78,686
w2	—	—	—	little	256(d) 64(w)	—	little	little	102(d) 97(w)	little		65,270
w3	130(d) 65(w)	101(d) 76(w)	140(d) 45(w)	142 (d) 100 (w)	90 (d) 51(w)	little	little	little	357(d) 142(w)	little		69,530
w4	little	477 (d) 167(w)	266 (d) 43(w)	444(d) 196 (w)	173 (d) 57(w)	—	little	423 (d) 731(w)	237(d) 132(w)	151(d) 81(w)		57,458
w5	—	—	—	little	127(d) 63(w)	161(d) 118 (w)	—	—	little	134(d) 65(w)	87.5 /MPa	133,640
w6	—	—	little	171 (d) 30(w)	little	339(d) 105 (w)	221(d) 106(w)	little	little	little		144,014
w7	little	76(d) 71(w)	—	—	194(d) 91(w)	little	253(d) 140(w)	little	little	115(d) 34(w)		165,836
w8	little	little	little	little	—	little	—	little	little	—		175,079
w9	142(d) 76(w)	—	134(d) 244(w)	220(d) 101(w)	285(d) 70(w)	little	192(d) 100(w)	176(d) 181(w)	97(d) 161(w)	little	65 /MPa	297,460
w10	299(d) 59(w)	little	182(d) 88(w)	54(d) 89(w)	206(d) 121(w)	239(d) 140(w)	158(d) 236(w)	74(d) 128(w)	148(d) 129(w)	—		356,915
w11	—	—	little	105(d) 15(w)	little	little	—	—	—	—		786,894
w12	—	—	little	—	145(d) 60(w)	little	little	little	—	—		512,609

4.1 Life Prediction of the corroded fatigue specimen with uniform section

Two kinds of software AFGROW and FASTRAN3.9 were used to predict the fatigue lives of the corroded material. In the predictions using AFGROW, the initial crack depth and length were assumed to be the corresponding average pit dimensions. However, because the ratio of pit depth to pit width is out of the range which can be accepted in FASTRAN3.9, an initial semi-circular crack was assumed in FASTRAN3.9 predictions herein, and its diameter was calculated according to average pre-corrosive pit dimensions and an area equivalent rule. Comparisons between tested and predicted fatigue lives using the two different methods for the corroded material with two immersion times are given in Fig.11(a, b), respectively. It should be mentioned that herein for AFGROW a non-interactive model was selected. From the figures, the predictions from two kinds of models agree reasonably with tests. In total, AFGROW seems to be better. The reason maybe is that the semicircular initial crack assumption decreased its capacity of the prediction for FASTRANII.

4.2 Life Prediction of the corroded panel with 5 collinear holes

Two kinds of methods were used to predict fatigue lives of the corroded panel with 5 collinear holes. One assumed that initial semi-circular surface cracks with the same size exist at each edge of the holes, and to perform prediction by means of FASTRAN3.9 directly. An interactive effect between the neighboring cracks in the process of crack growth does not be considered. Another considered effect of the interaction between the neighboring through cracks on stress intensity factor by the combination method of SIF calculation.

After the initial semi-circular surface cracks become the through cracks, according to Dowling [10], let the transition crack length is

$$a_t = \frac{r}{(11.2k_t)^2 - 1} \quad \text{.............................(1)}$$

Where r is radius of the hole, and k_t is the stress concentration factor at the edge of the hole.

When $a < a_t$,

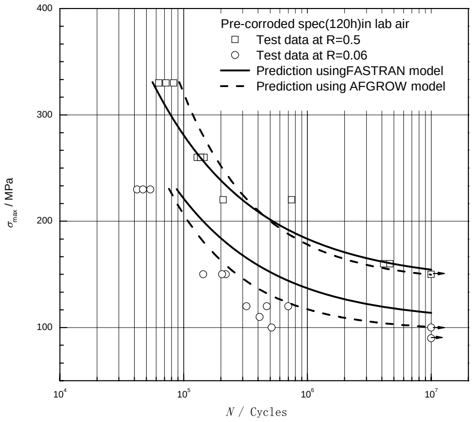

(a) For 120 h pre-corroded specs

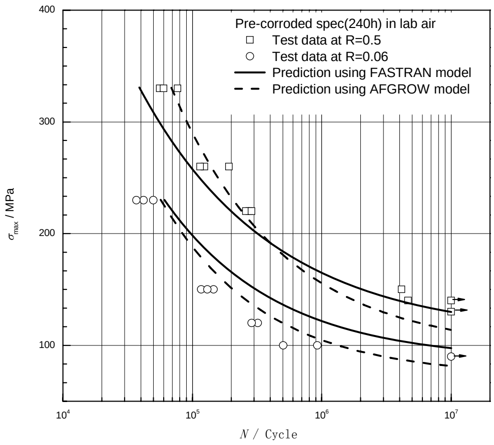

(b) For 240 h pre-corroded specs

Fig.11 Comparisons between tested and predicted fatigue lives for the corroded specs with different immersion times

$$K = B_{hs}\sigma\sqrt{\pi(a+r)} \ldots\ldots\ldots\ldots\ldots\ldots\ldots\ldots\ldots (2)$$

Where, $B_{hs} = B_h\sqrt{\dfrac{a}{a+r}} = \left(\dfrac{F_1}{F_2 + \dfrac{a}{a+r}} + F_3\right)\sqrt{\dfrac{a}{a+r}}$

For double cracks at the edges of the hole, $F_1 = 0.6865$、$F_2 = 0.2772$、$F_3 = 0.9439$.

When $a>a_t$ and the uncracked ligament between the neighboring cracks is greater than half of the distance between the neighboring holes,

$$K = B_w\sigma\sqrt{\pi(a+r)},\ where\quad B_w = \sqrt{\sec\left(\frac{\pi(a+r)}{w}\right)} \ldots (3)$$

Only the effect of panel width boundary is considered herein.

When the uncracked ligament between the neighboring cracks is less than a half of the distance between the neighboring holes, the interactive effect between the neighboring cracks must be considered. And,

$$K = B_w B_{Ia}\sigma\sqrt{\pi(a+r)} \ldots\ldots\ldots\ldots\ldots\ldots (4)$$

According to Kamei and Yokobori [11], for the interactive cracks as shown in Fig.12

$$B_{Ia} = \sqrt{1+\frac{2b}{l}}\left[1-(1+\frac{l}{2a})\frac{K(k)-E(k)}{K(k)}\right]$$

Where *K(k), E(k)* are the complete elliptic integrals of the first and the second kinds, respectively. a is that the crack length plus r. k is the geometry factor, and herein

$$k = 2\sqrt{\frac{a\cdot b}{(2a+l)(2b+l)}}$$

The initial semi-circular cracks with the same sizes were assumed to be at each edge of holes in the two kinds of predictions herein. The radius of the initial surface crack was calculated according to an average of pre-corrosive pit dimensions given in table 2 and an area equivalent rule. In the predictions, the da/dN-ΔK relationship data at R=0.06 as shown in Fig.8 were used to calculate crack increase amount Δa under given loading cycles for each crack at the edges of holes. The net section yielding criterion with the safe factor of 2 was used to judge the failure of the cracked panels.

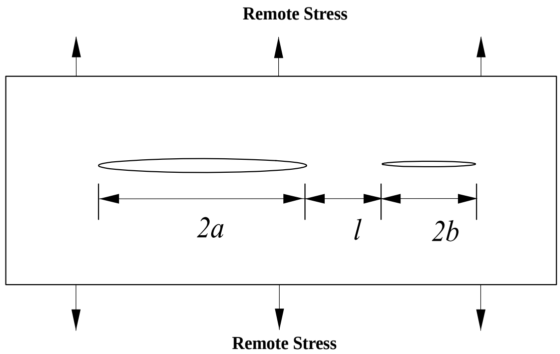

Fig.12 Interactive sketch map between two cracks

Comparison between tested and predicted fatigue lives for the corroded panels is shown in Fig.13. From the figure, it is found that the method considering the interaction effect of the neighboring cracks gives better prediction.

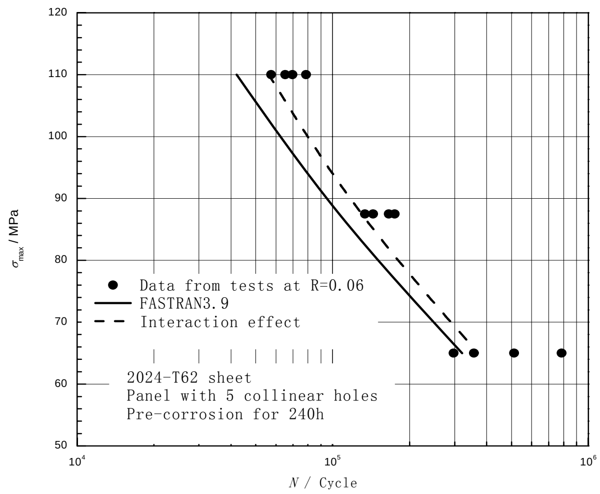

Fig.13 Comparison between tested and predicted fatigue lives for the corroded panels

5 Conclusions

(1) Average depth of prior-corrosion pit varies with immersion time in a power function relationship.

(2) Effect of prior corrosion on fatigue behavior of material specimen and panel with 5 collinear holes is obvious.

(3) Effect of prior corrosion is not found on crack growth behavior of both small and large crack growth, and that near physical small crack threshold regime.

(4) The effect of corrosive environment on large crack growth rate is small for the present material.

(5) Small cracks initiated naturally from the voids for non-corroded material. For pre-corroded material, small cracks initiated from pre-corrosive pits. For non-corroded material in lab air, an obvious small crack effect is found at R=-1, but it is not exist at R=0.06. For the corroded material in both lab air and aqueous 3.5% NaCl, the small crack effect is not found at R=-1 and 0.06.

(6) Both FASTRAN3.9 and AFGROW can be used to predict reasonably fatigue lives for pre-corroded specimen. For fatigue life prediction of the corroded panel with 5 collinear holes, the method considering the interaction effect of the neighboring cracks can give better prediction than the method using FASRTRAN3.9 directly.

References

[1] Medved J J, Breton M and Iring P E. Corrosion pit size distributions and fatigue lives—a study of the EIFS technique for fatigue design in the presence of corrosion. Int. J. Fatigue 26, pp71-80, 2004.

[2] DuQuesnay D L, et al. Fatigue crack growth from corrosion damage in 7075-T6511 aluminum alloy under aircraft loading. Int. J. Fatigue 25, p371, 2003.

[3] Rokhlin S I, Kim J Y, Nagy H and Zoofan B. Effect of pitting corrosion on fatigue crack initiation and fatigue life. Eng Fract Mech, 62, pp425-44,1999.

[4] Ishihara S, et al. Prediction of corrosion fatigue lives of aluminum alloy on the basis of corrosion pit growth. Fatigue Fract Engng Mater Struct, 29, pp472-480, 2006.

[5] Sankaran K K, et al. Effect of pitting corrosion on the fatigue behavior of aluminum alloy 7075-T6: modeling and experimental studies. Materials Science and Engineering, A297, pp223-229, 2001.

[6] Piascik P S, Willard S A.The growth of small corrosion fatigue cracks in alloy 2024. Fatigue Fract Engng Mater Struct, 17(11),pp1247-1259,1994.

[7] Newman J C, Wu X R, et al. Small-crack effects in high-strength aluminum alloys—NASA/CAE cooperative program, NASA RP-1309, 1994.

[8] Liu J Z, et al. Crack Growth behavior and fatigue life prediction based on worst-case near-threshold data of large crack for 9310 steel. Fatigue Fract Engng Mater & Struct, 25, pp467-480, 2002.

[9] Bray G H, et al. Effects of prior corrosion on the S/N fatigue performance of aluminum alloys 2024-T3 and 2524-T3, ASTM STP 1298, Philadelphia, p.89,1997.

[10] Dowling N E. Notched Member Fatigue Life Prediction Combining Initiation and Propagation. Fracture of Engng Mater and Struct, 2, pp 129,1979

[11] Kamei A., Yokobori T. Two collinear Asymmetrical Elastic Cracks. Report of the Research Institute for Strength and Fracture of Materials, Tohoku University, Vol.10, Section 1-4, pp 41-42, 1974

Contact Author: jianzhongliu09@sina.com

Copyright Statement